nature energy

SUPPLEMENTARY INFORMATION

ARTICLE NUMBER: 16066 | DOI: 10.1038/NENERGY.2016.66

Rational design of redox mediators for advanced Li-O_2 batteries

Hee-Dae Lim,[1,†] Byungju Lee,[1,†] Yongping Zheng,[2] Jihyun Hong,[1] Jinsoo Kim,[1] Hyeokjo Gwon,[3] Youngmin Ko,[1] Minah Lee,[5] Kyeongjae Cho,[,2,6] and Kisuk Kang[*,1,4]*

1 Department of Materials Science and Engineering, Research Institute of Advanced Materials (RIAM), Seoul National University, 1 Gwanak-ro, Gwanak-gu, Seoul 151-742, Republic of Korea

2 Department of Mechanical & Aerospace Engineering, Seoul National University, 1 Gwanak-ro, Gwanak-gu, Seoul 151-742, Republic of Korea

3 Energy Lab, Material Research Center, Samsung Advanced Institute of Technology, Samsung Electronics Co., Ltd., 130 Samsung-ro, Yeongtong-gu, Suwon-si, Gyeonggi-do 16678, Republic of Korea

4 Center for Nanoparticle Research, Institute for Basic Science (IBS), Seoul National University, 1 Gwanak-ro, Gwanak-gu, Seoul 151-742, Republic of Korea

5 Chemical Engineering Department, Stanford University, Shriram Center, 443 Via Ortega, Stanford, CA 94305-4125, USA

6 Department of Materials Science and Engineering, University of Texas, Dallas, Richardson, TX 75080, USA

† These authors contributed equally to this work.

* Corresponding author: matlgen1@snu.ac.kr, kjcho@utdallas.edu

DOI: 10.1038/NENERGY.2016.66

SUPPLEMENTARY FIGURES

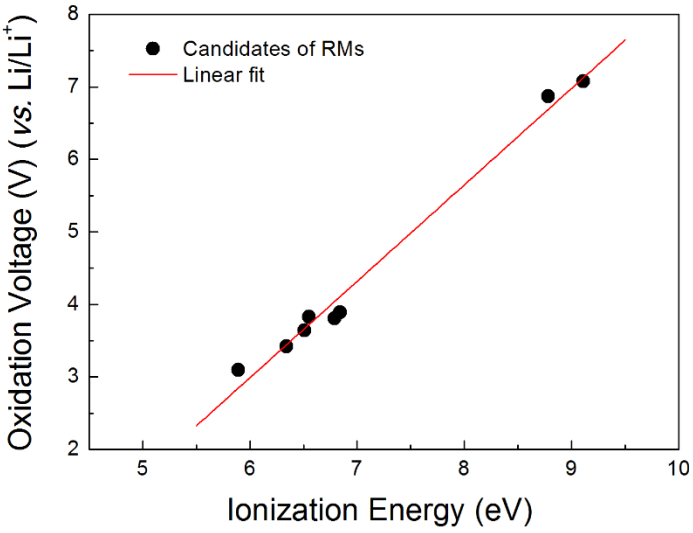

Supplementary Figure 1. Relationship between ionization energy in a vacuum and oxidation voltage (*vs.* Li/Li^+) in TEGDME electrolyte for the RM candidates described in Table 1.

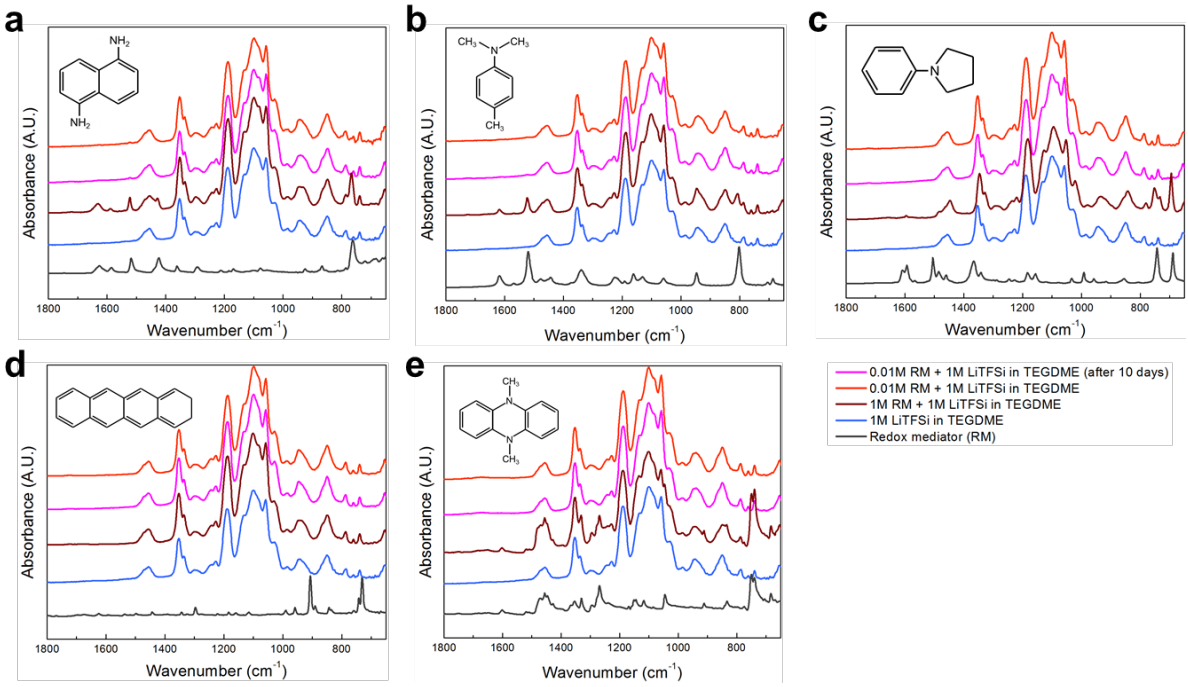

Supplementary Figure 2. FT-IR spectra of (a) NDA, (b) TMA, (c) PPD, (d) NC, and (e) DMPZ in the range of 1800–650 cm^{-1}. The spectra were obtained after dissolving the RMs in TEGDME. All the RMs were well dissolved in TEGDME and stable even after 10 days. Although NC was not identified after its dissolution in the electrolyte, the electrolyte exhibited no changes and appeared to be stable.

DOI: 10.1038/NENERGY.2016.66

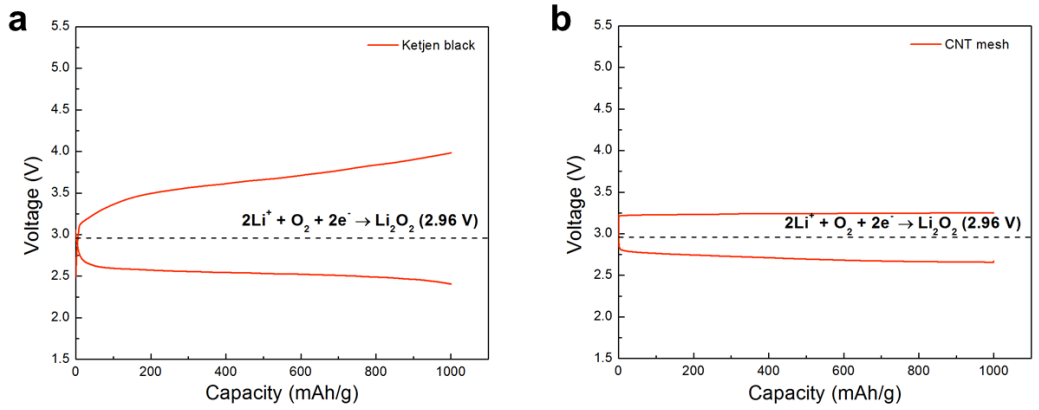

Supplementary Figure 3. The first discharge and charge profiles of Li-O_2 cells using a) Ketjen black electrode with LiI catalyst and b) carbon nanotube mesh electrode with LiI catalyst. The discharge capacity is limited to 1000 $mAhg^{-1}$, and the current density is 200 mA g^{-1}. Even if the Li-O_2 cells used the same soluble catalyst of LiI, the charge profiles were different based on the types of air cathodes used. A slight deviation of the charge profile is observed in the cell using the bulk carbon of Ketjen black because of the transport limitations of the catalyst and reaction products, whereas constant charge potential was observed using the hierarchically porous carbon nanotube mesh electrode.

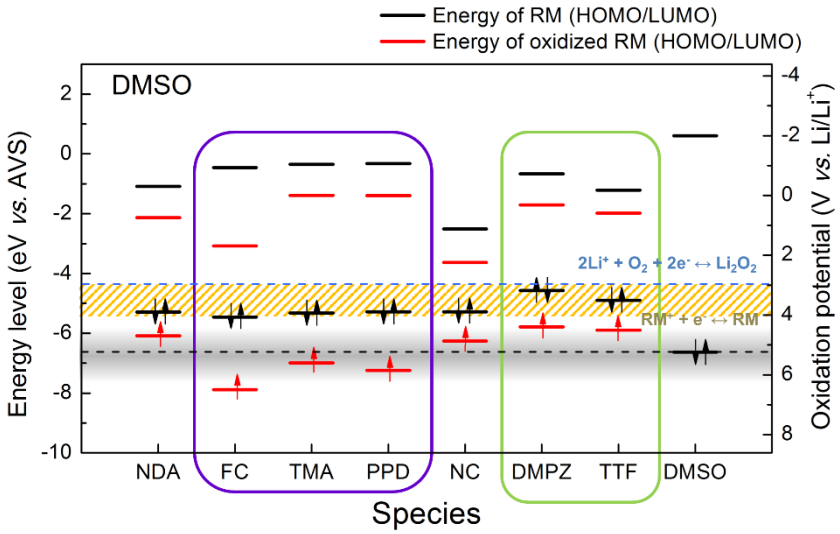

Supplementary Figure 4. HOMO and LUMO energies of original RMs (black line) and first oxidized RMs (red line) in DMSO electrolyte using DFT calculations. The dotted blue and black lines represent the theoretical formation energy of Li_2O_2 and the HOMO energy of DMSO, respectively.

DOI: 10.1038/NENERGY.2016.66

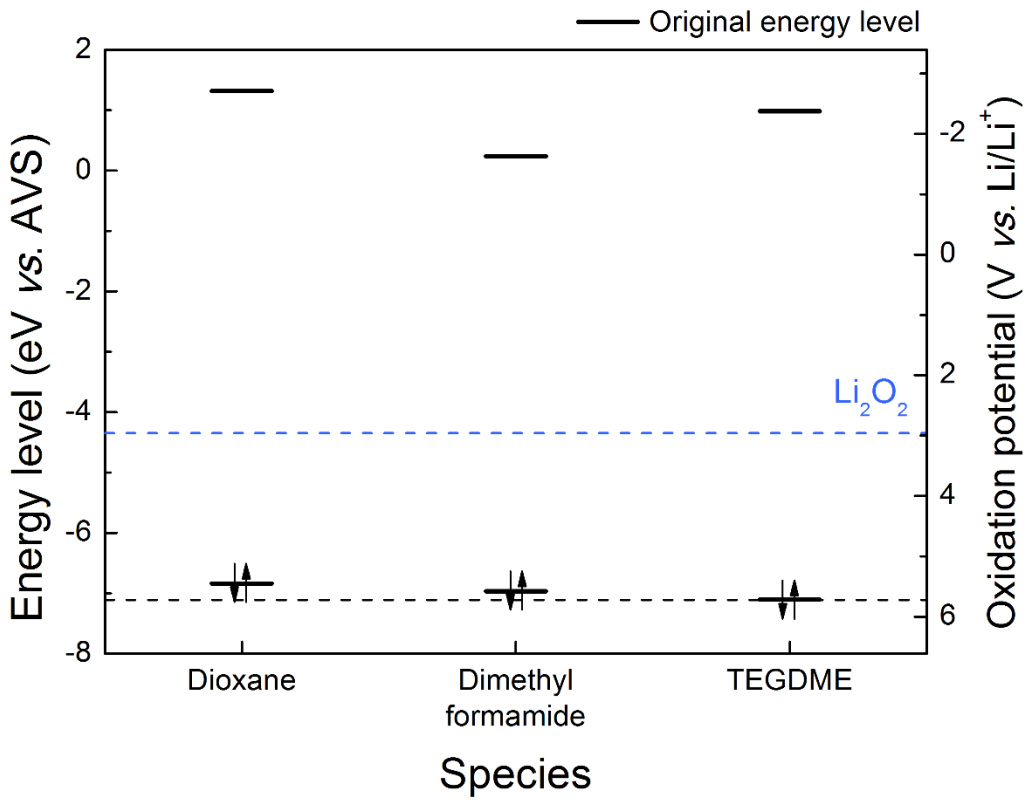

Supplementary Figure 5. HOMO and LUMO energies of 1,4-dioxane and N,N-dimethylformamide in TEGDME electrolyte using DFT calculations. 1,4-dioxane and N,N-dimethylformamide have high I.E. values of ~6.8 and ~6.9 eV in TEGDME, respectively, which are quite high compared with those of the other RM candidates described in Figure 4. Therefore, it is believed that these molecules are not oxidized under a typical voltage window (2.0–4.5 V), as demonstrated in Figure 2c.

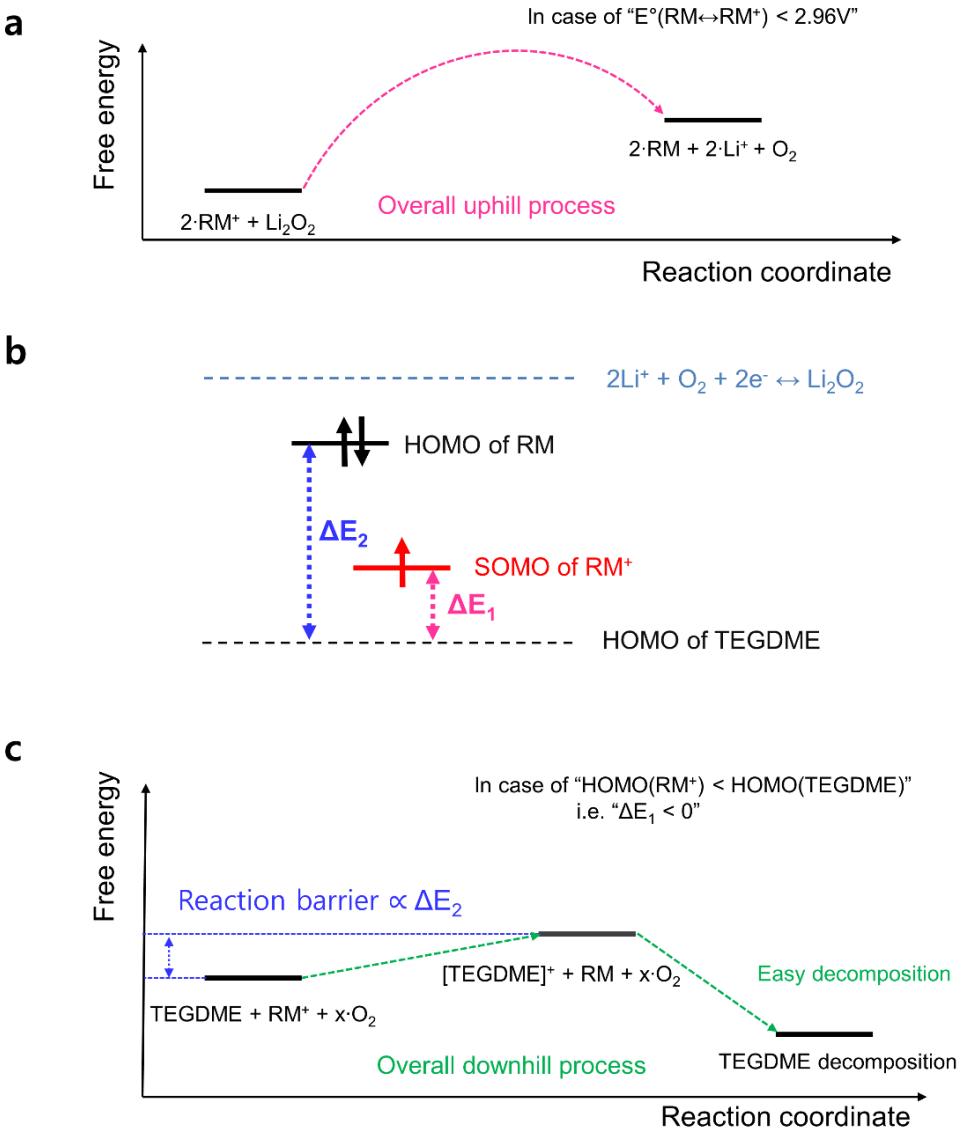

Supplementary Figure 6. Schematic energy diagram of (a) $2RM^{+} + Li_2O_2 \leftrightarrow 2RM + 2Li^{+} + O_2$ reaction in case of $E°(RM \leftrightarrow RM^{+}) < 2.96$ V (b) relative MO position of RM/TEGDME, and (c) TEGDME decomposition reaction in the presence with RM^{+} whose HOMO is lower than that of the solvent. See Supplementary Note 1 for detailed discussion.

DOI: 10.1038/NENERGY.2016.66

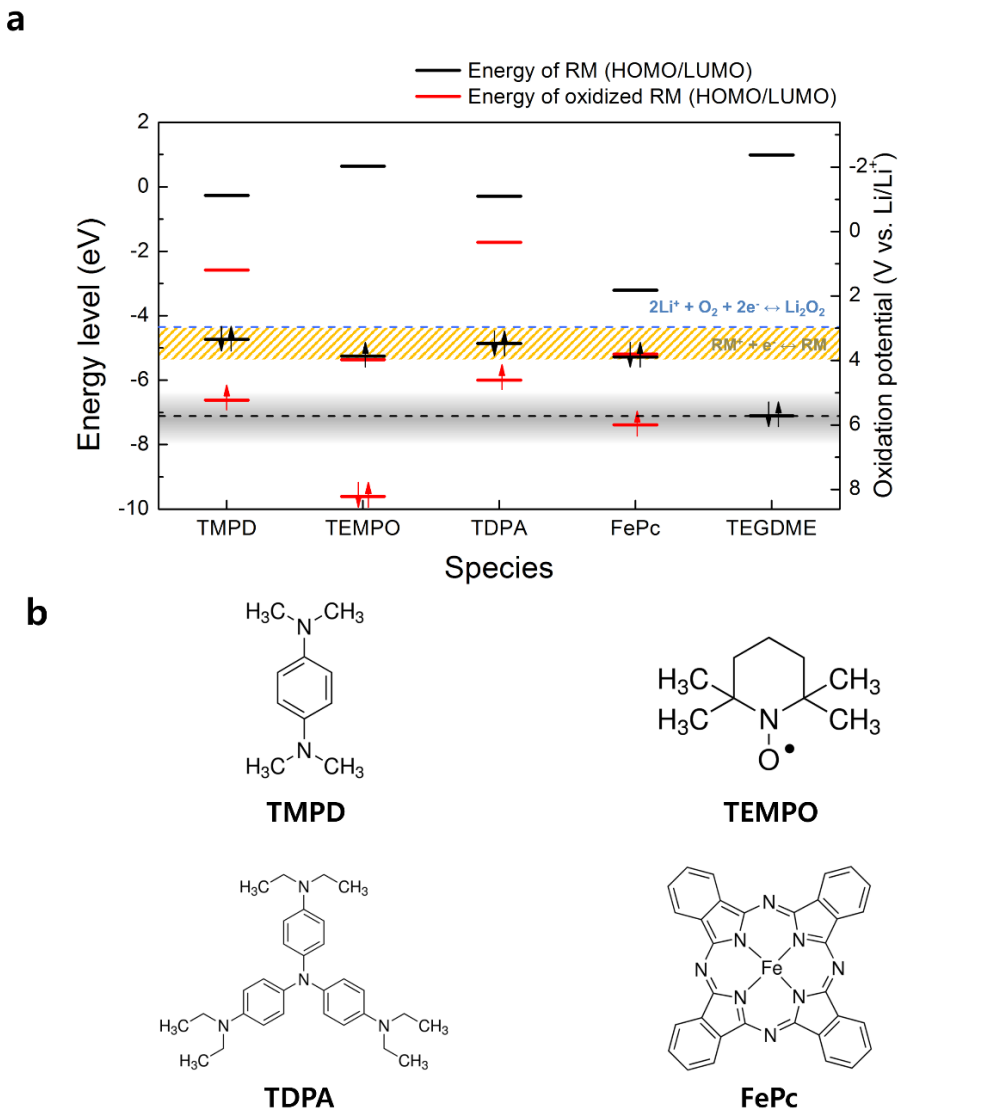

Supplementary Figure 7. (a) HOMO and LUMO energies and (b) molecular structures of TMPD, TEMPO, TDPA and FePc in TEGDME electrolyte based on DFT calculations. See Supplementary Note 2 for detailed discussion.

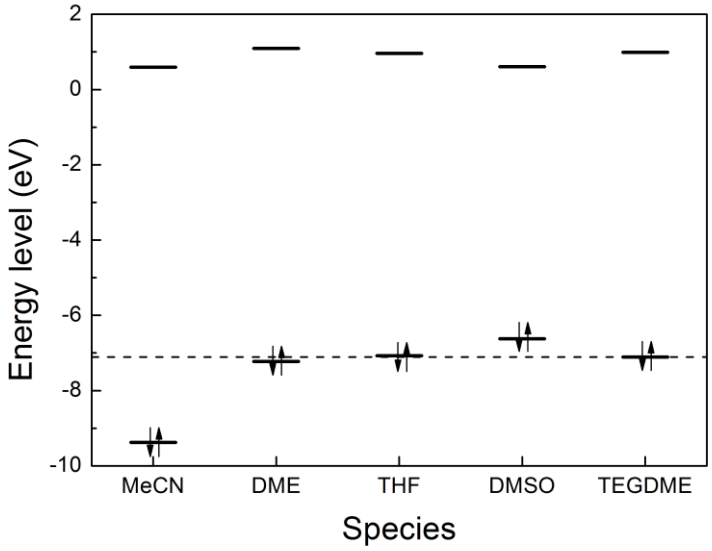

Supplementary Figure 8. The HOMO/LUMO energies of five representative solvents used in the Li-O_2 battery. See Supplementary Note 3 for detailed discussion.

DOI: 10.1038/NENERGY.2016.66

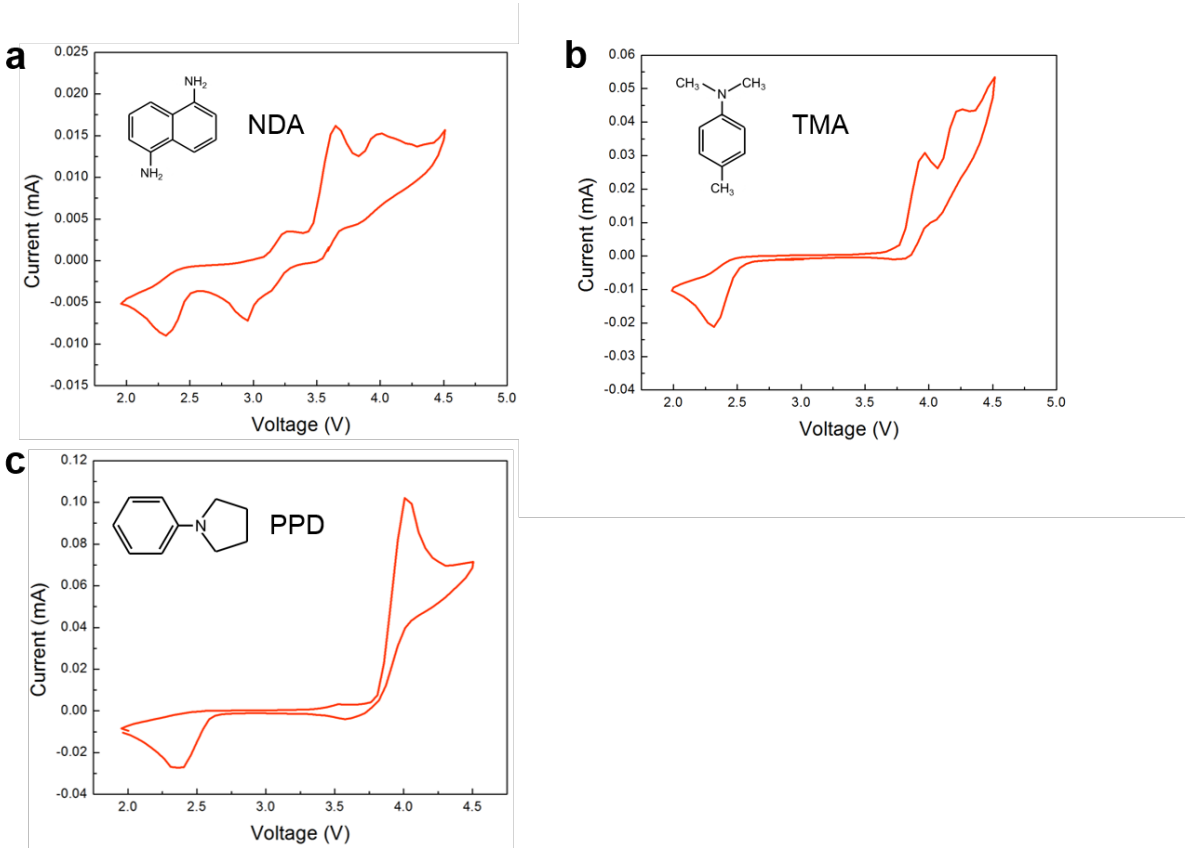

Supplementary Figure 9. CV of (a) NDA, (b) TMA, and (c) PPD in 0.1 M TBATFSI/DMSO under Ar atmosphere at a scan rate of 100 mV s^{-1}. In total, 1 mM of the RMs was added to the electrolyte.

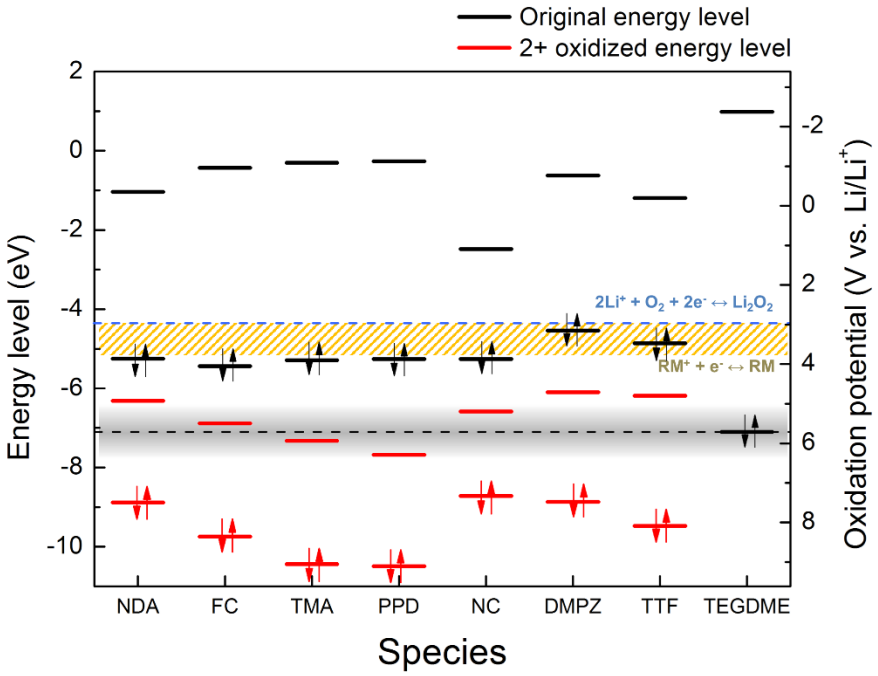

Supplementary Figure 10. HOMO and LUMO energies of original RMs (black line) and second oxidized RMs (red line) in TEGDME electrolyte based on DFT calculations. See Supplementary Note 4 for detailed discussion.

DOI: 10.1038/NENERGY.2016.66

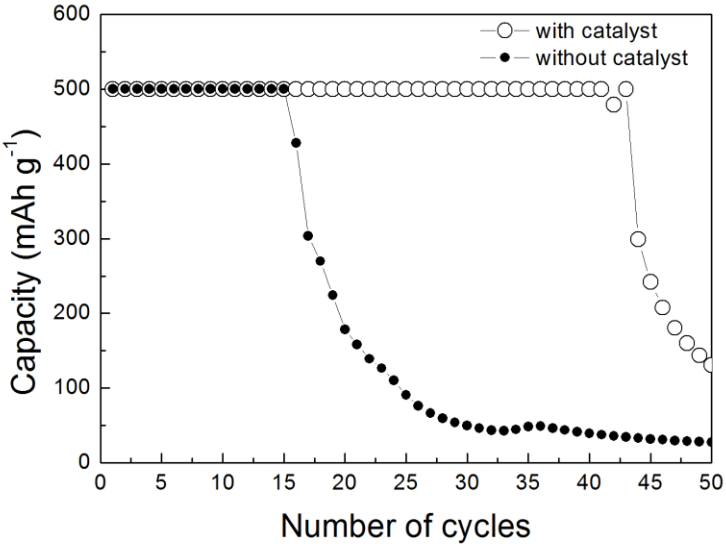

Supplementary Figure 11. Cyclability of the Li-O_2 cells with and without DMPZ catalyst. The capacity is limited to 500 mAh g^{-1} at a constant current of 0.2 mA cm^{-2} in an oxygen atmosphere. See Supplementary Note 5 for detailed discussion.

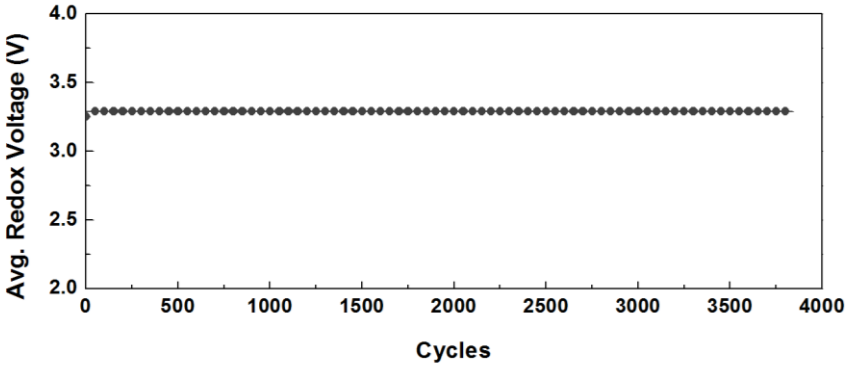

Supplementary Figure 12. Average redox voltage of DMPZ/DMPZ$^+$ along with the cycle numbers. The scan rate was constantly maintained at 100 mV s^{-1}. We investigated the stability of DMPZ/DMPZ$^+$ redox under the prolonged cycles. Supplementary Fig. 12 shows that the redox potentials of DMPZ/DMPZ$^+$ is highly stable for a few thousands cycles. Average redox voltages of DMPZ/DMPZ$^+$ are constantly maintained, which implies that the redox of DMPZ/DMPZ$^+$ is reversible and stable.

DOI: 10.1038/NENERGY.2016.66

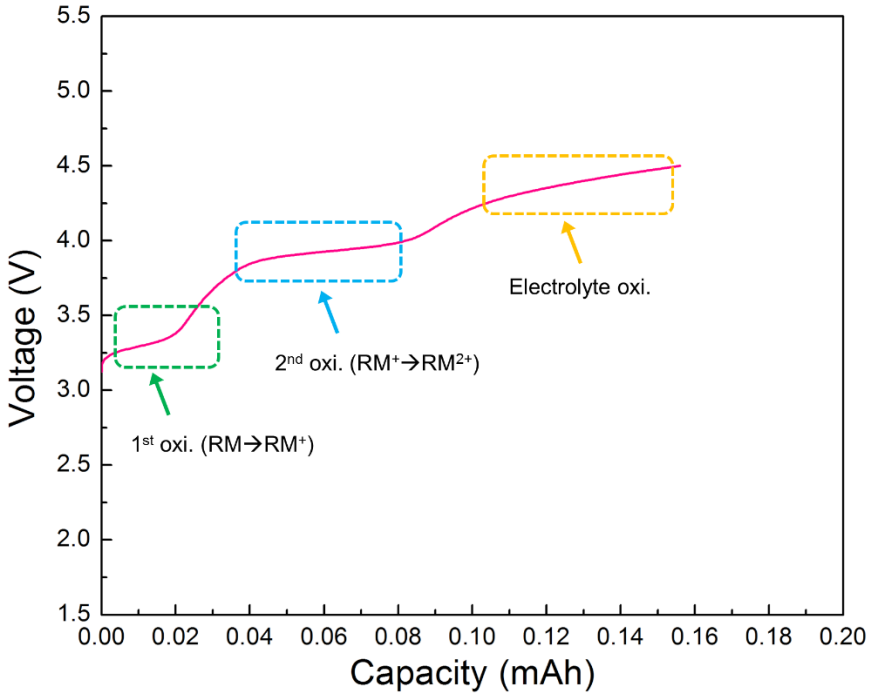

Supplementary Figure 13. Electrochemical oxidation of DMPZ to 4.5 V in TEGDME electrolyte. The theoretical capacity that DMPZ alone can contribute by the oxidation to $DMPZ^+$ and $DMPZ^{2+}$ in the absence of Li_2O_2 is approximately 0.1 mAh based on the amount of RMs used in the Li-O_2 cell. Accordingly, the capacity from the intrinsic DMPZ oxidation is close to 0.1 mAh, as shown in Supplementary Fig. 13, followed by the electrolyte oxidation in the continuing charge over 4.2 V. Considering that the capacity of the Li-O_2 cell in Figure 2c is 1 mAh, which is 10 times higher than the possible capacity from RM, the charge capacity with the low overpotential in Figure 2c clearly demonstrates a continuous and simultaneous reduction of $DMPZ^+$ to DMPZ by reacting with Li_2O_2 during the charge process.

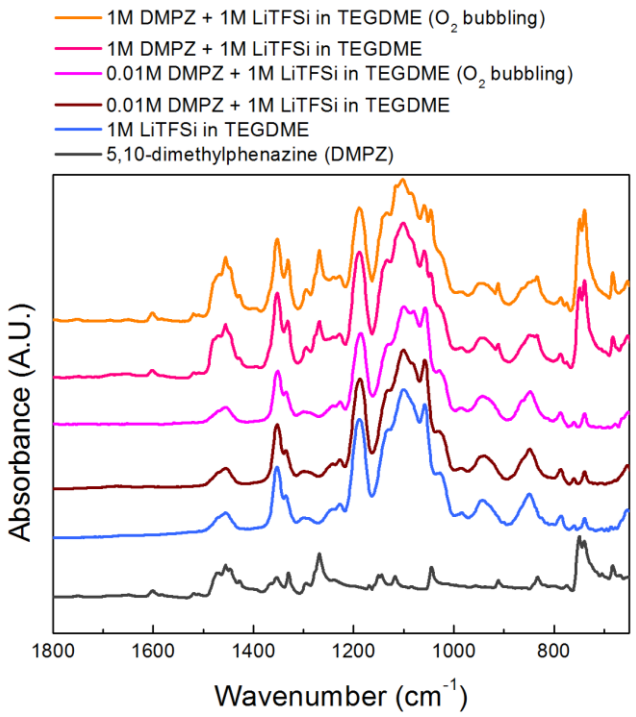

Supplementary Figure 14. FT-IR spectra of DMPZ in the range of 1800–650 cm^{-1}. The spectra were obtained after dissolving the RMs in TEGDME electrolyte with Ar and O_2 bubbling. The stability of DMPZ in the presence of oxygen was first examined with 0.01M and 1M concentration of DMPZ in TEGDME-based electrolyte. We dissolved DMPZ in the electrolyte and bubbled with O_2 for 1 hour before carrying out FTIR measurements. Supplementary Fig. 14 shows that there is no dominant change in the peaks from both DMPZ and electrolyte, which indicates the stability of DMPZ with the oxygen in the electrolyte.

DOI: 10.1038/NENERGY.2016.66

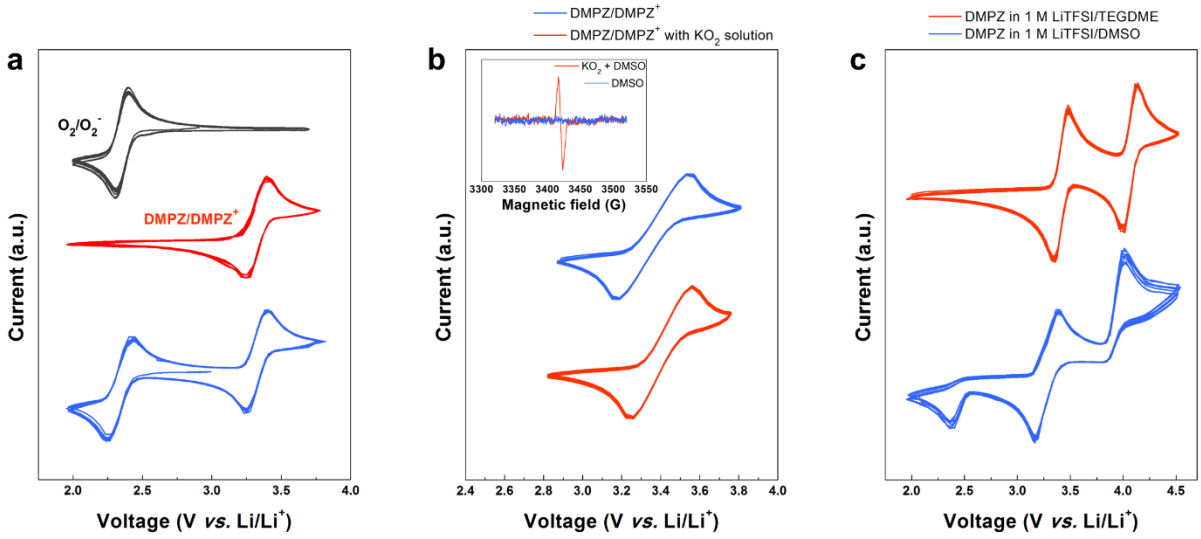

Supplementary Figure 15. a) Cyclic voltammogram of oxygen alone (black), DMPZ with no oxygen present (red), and DMPZ (blue) under an O_2 atmosphere in TEGDME electrolyte. b) Cyclic voltammogram of DMPZ in DMSO electrolyte without (blue) and with (red) the chemically synthesized oxygen radicals. (Inset: ESR signal of the chemically generated oxygen radicals.) c) Cyclic voltammogram of DMPZ in different electrolytes of TEGDME and DMSO under an Ar atmosphere. The three electrodes compose of Pt counter and gold working electrodes with Ag/Ag^+ in acetonitrile solution as a reference electrode. The scan rate was maintained at 100 mV s^{-1}. See Supplementary Note 6 for detailed discussion.

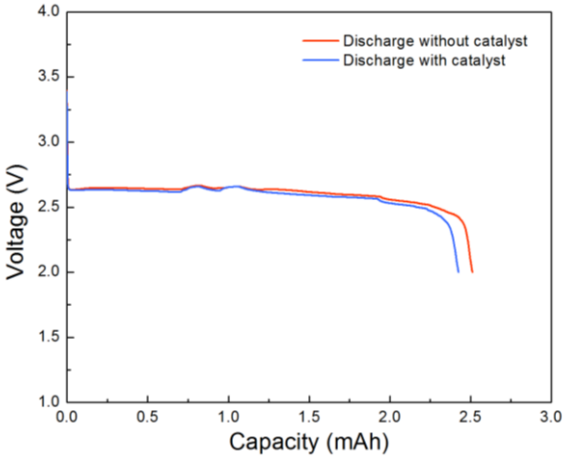

Supplementary Figure 16. Discharge profiles of the cells with and without DMPZ catalyst in an oxygen atmosphere at a constant rate of 0.2 mA/cm^2. See Supplementary Note 7 for detailed discussion.

DOI: 10.1038/NENERGY.2016.66

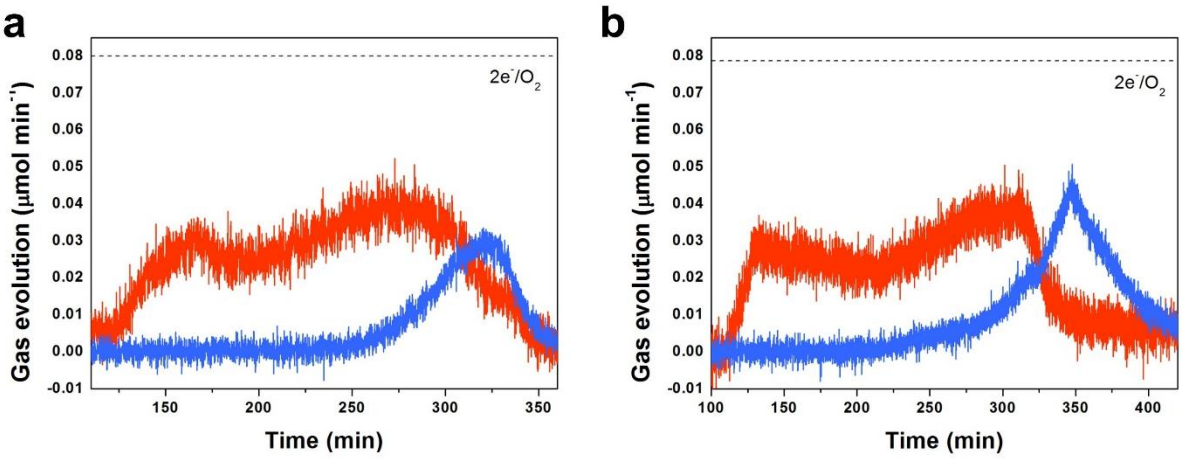

Supplementary Figure 17. DEMS results of Li-O_2 cells during charge (a) with and (b) without DMPZ catalyst. Each cell was discharged to 1mAh and recharge to the same capacity at a current density of 0.2 mA cm^{-2}. See Supplementary Note 8 for detailed discussion.

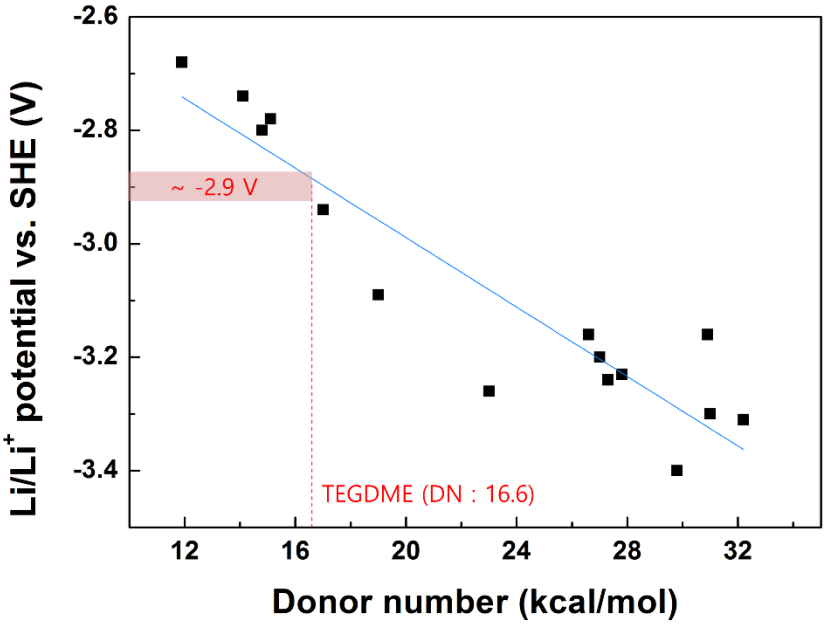

Supplementary Figure 18. Relationship between donor number of various non-aqueous solvents and Li/Li^+ redox potential *vs*. SHE in each solvent. While the redox potential of Li/Li^+ *vs*. SHE in TEGDME electrolyte was not precisely reported, it can be derived from the relationship between the donor number of solvent and Li/Li^+ redox potential in each solvent. The redox potential of Li/Li^+ *vs*. SHE in TEGDME can be interpolated to around -2.9 V, which is similar to that in water. See Supplementary Note 9 for detailed discussion.

DOI: 10.1038/NENERGY.2016.66

SUPPLEMENTARY TABLES

Supplementary Table 1. Donor number of various non-aqueous solvents and Li/Li^+ redox potential *vs*. SHE in each solvent.

Solvent	Donor number[1] (kcal/mol)	Li/Li^+ redox potential vs. SHE[2] (V)
Benzonitrile	11.9	-2.68
Acetonitrile	14.1	-2.74
Tetramethylenesulfone	14.8	-2.8
Propylene carbonate	15.1	-2.78
Acetone	17	-2.94
Methanol	19	-3.09
Trimethyl phosphate	23	-3.26
N,N-dimethylformamide	26.6	-3.16
N-methylformamide	27	-3.2
1-methyl-2-pyrrolidinone	27.3	-3.24
N,N-dimethylacetamide	27.8	-3.23
Dimethylsulfoxide	29.8	-3.4
N,N-diethylformamide	30.9	-3.16
N,N,N,N-tetramethylurea	31	-3.3
N,N-diethylacetamide	32.2	-3.31

Supplementary Table 2. Experimental and calculated redox potential of RM candidates. See Supplementary Note 9 for detailed discussion.

Molecules	Redox potential from I.E. calculation (a) (*vs.* Li/Li$^+$)	Redox potential from HOMO level calculation (b) (*vs.* Li/Li$^+$)	Redox potential from experiment (c) (*vs.* Li/Li$^+$)	ΔE (c)-(a)	ΔE (c)-(b)	ΔE (a)-(b)
PPD	3.89	3.87	4.0	0.11	0.13	0.02
TMA	3.82	3.90	3.9	0.08	0	-0.08
NDA	3.65	3.86	3.6	-0.05	-0.26	-0.21
DMPZ	3.11	3.15	3.3	0.19	0.15	-0.04
TTF	3.43	3.47	3.6	0.17	0.13	-0.04
TMPD	3.09	3.35	3.3	0.21	-0.05	-0.26

DOI: 10.1038/NENERGY.2016.66

SUPPLEMENTARY NOTES

Supplementary Note 1. Reaction energetics of RM, Li_2O_2 and TEGDME.

The catalytic activity of RM is determined by the relative HOMO energy state of RM not that of RM^+ *vs.* the oxidation potential of Li_2O_2. It is because, when the redox potential of $RM \leftrightarrow RM^+ + e^-$ is lower than that of $Li_2O_2 \leftrightarrow 2Li^+ + O_2 + 2e^-$ (*i.e.* the formation of Li_2O_2 is thermodynamically more favorable than the reduction of RM^+), the decomposition of Li_2O_2 via the reduction of RM^+ is the uphill process in the overall energy scale of the reaction. As schematically depicted in Supplementary Fig. 6a, even if SOMO level of RM^+ is located below the Li_2O_2 energy, thus, the electron prone to be transferred from Li_2O_2 to RM^+ reducing to RM and oxidizing Li_2O_2, the overall energy of products ($2RM + 2Li^+ + O_2$) becomes higher than the reactants ($2RM^+ + Li_2O_2$) simply because the formation of Li_2O_2 is thermodynamically more favorable than the reduction of RM^+ (*i.e.* redox potential of $RM \leftrightarrow RM^+ + e^-$ is lower than that of $Li_2O_2 \leftrightarrow 2Li^+ + O_2 + 2e^-$). In this respect, the decomposition of Li_2O_2 should not occur if the oxidation potential of RM is below the energy level of Li_2O_2.

The situation is slightly different in the case of TEGDME decomposition as shown in Supplementary Fig. 6b-c. In Supplementary Fig. 6b, the relative position of HOMO of RM^+ (and RM) *vs.* that of TEGDME is denoted as ΔE_1 and ΔE_2, respectively, for the clarity of the discussion. When the ΔE_1 is positive, i.e. the HOMO of RM^+ lies above that of TEGDME, the decomposition of TEGDME does not occur due to the absence of electron transfer as mentioned in the main text. Let us consider the case that ΔE_1 is negative and ΔE_2 is positive. In this case, the reduction of RM^+ would increase the overall energy of the system similar to the case above (if the electron transfer from TEGDME to RM^+ occurs). However, it should be noted that the oxidation of TEGDME molecules easily triggers sequential side reactions

leading to the decomposition of the electrolyte, thus the process does not go back to the initial condition. It is well known that the solvents in Li-O_2 cells is highly vulnerable to H-abstraction and nucleophilic attack of oxygen radical and upon the oxidation of solvents they become more vulnerable triggering sequential side reactions[J. Phys. Chem. Lett. 5, 2419 (2014)][J. Phys. Chem. Lett. 3, 3043 (2012)][J. Electrochem. Soc. 160, A160 (2013)][Chem. Phys. Lett. 588, 42 (2013)][J. Phys. Chem. A 115, 12399 (2011)]. Especially in the presence of O_2 in the cell, it is expected that the decomposition of TEGDME can readily occur by the nucleophilic attack of oxygen molecule or radicals.

One thing that should be noted, nevertheless, is that the temporary increase of the energy in the intermediate state plays a role of kinetic barrier of the TEGDME decomposition as depicted in Supplementary Fig. 6c. As discussed above, the uphill energy is proportional to how far the HOMO level of RM is located from the oxidation potential of TEGDME. (i.e. ΔE_2) In this respect, the higher ΔE_2 is, the more resistant to the TEGDME decomposition. On the other hand, if ΔE_2 is too large so that the HOMO level lies above the Li_2O_2 potential, the RM is not active. It implies that the HOMO level of RM should be more carefully considered and it can be the indirect descriptor for the stability of RM with respect to the electrolyte.

DOI: 10.1038/NENERGY.2016.66

Supplementary Note 2. Stability of TMPD, TEMPO, TDPA and FePc.

The HOMOs of all four molecules in neutral state were lower than electron energy of Li_2O_2 formation, implying that all the molecules are capable of decomposing Li_2O_2 in the oxidized form. We also examined the stability of the four molecules as following. As mentioned in the manuscript, although the HOMO of $TMPD^+$ is slightly higher than HOMO of TEGDME, $TMPD^+$ can decompose TEGDME because the HOMO of $TMPD^+$ is located in the vicinity of HOMO of TEGDME (grey region). It corresponds well with the previous paper reporting the low efficiency of TMPD compared to that of TTF[Net. Chem. 5, 489 (2013)]. In the case of TEMPO, it has a partially filled HOMO state in the neutral state unlike other RMs, thus, the HOMO of $TEMPO^+$ is fully occupied. It indicates that it can be stable against the TEGDME oxidation even though the HOMO of $TEMPO^+$ lies below that of TEGDME due to the lack of the available energy state in the HOMO of $TEMPO^+$. Accordingly, experimentally it was reported that TEMPO decomposes Li_2O_2 efficiently[J. Am. Chem. Soc. 136, 15054 (2014)]. TDPA is also predicted to be stable in TEGDME when oxidized, because the HOMO of $TDPA^+$ is higher than the HOMO of TEGDME, which also agrees well with experimental result[ACS Cent. Sci. 1, 510 (2015)]. In case of FePc, the HOMO of $FePc^+$ was predicted to be lower than the HOMO of TEGDME, however, the experiments reported a high cycle stability (~135 cycles) of Li-O_2 cell with FePc mediator[J. Am. Chem. Soc. 136, 8941 (2014)]. We attribute the discrepancy to the reaction mechanism of FePc. When charged, $FePc^+$ was reported to react with $(O_2)^{2-}$ ion, immediately forming $(FePc\text{-}O_2)^-$ complex, then oxidize into FePc and O_2. These multi-step reactions cannot be predicted by our methodology, which should be studied further in the future.

Supplementary Note 3. Stability of RM with different solvents.

We selected five representative solvents used in Li-O_2 batteries and calculated their MO energies as shown in Supplementary Fig. 8. Except for the DMSO case, the HOMOs of solvents were calculated to be lower than that of TEGDME, which implies that MeCN, DME and THF are more stable from RM^+ attack than TEGDME and DMSO is less stable. Although the HOMO of DMSO is higher than that of TEGDME, the relative location of the HOMO of RM^+ with respect to the HOMO of DMSO is not significantly changed compared to the case of TEGDME. (Supplementary Fig. 4) It is because the HOMO level of RM^+ is also affected by the choice of solvent due to the different dielectric constant of the solvent, and the HOMO levels of RM^+s are all upshifted in the DMSO. Therefore, the stability of DMSO against RM^+ would be only slightly inferior to the TEGDME case.

DOI: 10.1038/NENERGY.2016.66

Supplementary Note 4. Stability of RM^{2+} with TEGDME.

The stability of an RM is determined by the relative energy level of the RM^{+} with respect to that of the electrolyte, however, it should be noted that the electron transfer from the high energy state to the low energy state (from electrolyte to RM^{+}) can occur only when there is an available energy state present in the electron accepting molecule. In Figure 4, HOMO levels of all the RM^{+}s have unpaired electron in the state, thus are capable of accepting the electron from the electrolyte. In this respect, the stability of RMs with fully occupied HOMO level should be carefully considered. In Supplementary Fig. 10, we plotted the molecular orbital (MO) energy diagram of the RM^{2+} including $DMPZ^{2+}$ with respect to the TEGDME. The HOMO level of $DMPZ^{2+}$ lies below that of the electrolyte (lower than -9 eV *vs.* AVS). However, the electron transfer from the electrolyte to the HOMO level of $DMPZ^{2+}$ is not possible because the HOMO level is fully filled. Instead, the LUMO level of $DMPZ^{2+}$ is unoccupied and available, however, it lies above the energy level of the TEGDME. Thus the $DMPZ^{2+}$ can stay stable in TEGDME.

Supplementary Note 5. Cyclabilities of the cells with and without DMPZ.

The comparison of cyclabilities of the cells with and without DMPZ are presented in Supplementary Fig. 11. Interestingly, the cycle stability could be enhanced by about three times with the use of DMPZ catalyst at the same charge/discharge protocol using the carbon air electrode. The enhanced cyclability is attributable to the decreased charge polarization and the reduced CO_2 evolution due to the use of DMPZ catalyst, which successfully oxidizes Li_2O_2 by maintaining the low charging potential with minor side reactions. Nevertheless, the formation of unwanted discharge products, self-consuming of RMs in the anode side and the shuttle reaction need to be addressed for higher cycle stability.

DOI: 10.1038/NENERGY.2016.66

Supplementary Note 6. The stability of DMPZ with reduced oxygen species.

The stability of DMPZ with reduced oxygen species was also investigated by comparing the electrochemical activities of DMPZ/$DMPZ^+$ with and without oxygen radicals present by solution-based cyclic voltammetry (CV) as shown in Supplementary Fig. 15. Supplementary Fig. 15a shows the CV profile of O_2/O_2^- redox (black) and DMPZ/$DMPZ^+$ in an Ar atmosphere (red), which shows their characteristic anodic/cathodic peaks. The CV of DMPZ under an oxygen atmosphere (blue) in the same figure demonstrates that the redox of DMPZ/$DMPZ^+$ is still reversible and stable accompanying the redox of O_2/O_2^-. It suggests that the redox of DMPZ is stably maintained even with the redox reaction of O_2/O_2^- in the electrolyte. In order to further demonstrate the stability of DMPZ to oxygen radicals, we chemically generated O_2^- in DMSO electrolyte and tested the redox activity of DMPZ/$DMPZ^+$ as shown in Supplementary Fig. 15b. Oxygen radicals were chemically synthesized in the electrolyte using KO_2 powder based on the previous reports, [Phys. Chem. Chem. Phys. 15, 11830 (2013)] [Chem. Mater. 26, 4757 (2014)] and the chemically generated oxygen radicals were clearly detected by ESR measurement in the inset of Supplementary Fig. 15b. Supplementary Fig. 15b also confirms that the redox activity of DMPZ/$DMPZ^+$ (red) is almost unaltered with respect to the reference (blue) suggesting a stable redox of DMPZ in the reductive atmosphere. (DMSO solvent was used in this experiment because it has been reported as a relatively stable electrolyte for oxygen radicals, and it could dissolve KO_2 well[Phys. Chem. Chem. Phys. 15, 11830 (2013)].)

The stability of DMPZ was further inspected according to the types of electrolytes with different nucleophilic characters; DMSO (donor number 29.8) and TEGDME (donor number 16.6). As shown in the Supplementary Fig. 15c, the first and second redox reactions of

DMPZ in TEGDME are highly reversible. On the other hand, those in DMSO are not fully reversible, while the first redox reaction is relatively stable in consistent with the Supplementary Fig. 15b. The cathodic peak from the second redox reaction of DMPZ in DMSO electrolyte disappears and new cathodic peak around 2.4 V arises. (Such cathodic peaks around 2.4V is commonly observed in the electrolyte system that suffers from proton-involving side reactions[Z. Anal. Chem. 224, 184 (1966)].) The irreversibility of second redox reaction of DMPZ in DMSO is attributed to a strong nucleophilic attack of the solvent with high donor number (29.8) and can affect the reversibility of RM. [Mamantov, G. & Popov, A. I. Chemistry of Nonaqueous Solutions. VCH, New York, 227-276 (1994)] The demethylation of DMPZ at the second oxidation leads to a loss of its relevant reduction, and new peak around 2.4 V is attributable to a formed 5-methylphenazinium type product. [Z. Anal. Chem. 224, 184 (1966)] In this respect, when using DMPZ and utilizing the second redox reaction in Li-O_2 cells, TEGDME is preferred to DMSO electrolyte.

DOI: 10.1038/NENERGY.2016.66

Supplementary Note 7. Effect of DMPZ on discharge process of the Li-O_2 cell.

We measured the amount of evolved oxygen gas during charging by *in situ* DEMS (Differential Electrochemical Mass Spectroscopy) analysis. In the DEMS setup, Mass spectrometer (MS) (HPR-20, Hiden Analytical) and a potentio-galvanostat (WonA Tech, WBCS 3000, Korea) were combined. (The detail setup is described in previous reports. [Electrochim. Acta 90, 63 (2013)] [ACS Nano 8, 12483-12493 (2014)]) Before the gas analysis for the charging process, same discharge protocols were applied to cells with and without DMPZ. In Supplementary Fig. 16, the discharge capacities and profile shapes are shown for the two cells, which are almost similar regardless of the use of DMPZ and indicate that DMPZ has little influence during a discharge process. For the precise comparison, the discharge/charge capacity was limited to 1 mAh for the two cells which theoretically correspond to 18.6 μ mole of O_2 evolution during charging.

Supplementary Note 8. Gas analysis for the Li-O_2 cell with and without DMPZ.

Supplementary Fig. 17 shows the DEMS result for the two cells with concurrent O_2 and CO_2 evolution during the charging. The measured oxygen evolution efficiency is found to be almost similar to each other; the cell with DMPZ shows 5.76 e^-/O_2 (6.47 μ mole) and the cell without catalyst shows 5.66 e^-/O_2 (6.59 μ mole). While the efficiency of DMPZ decomposing pure Li_2O_2 in the electrolyte with 2.08 e^-/O_2 was clearly demonstrated in Figure 3 in the manuscript, much less efficiency was observed for both cells. It indicates that the formation of Li_2CO_3 or carbonate-based byproducts that decomposes and evolves CO_2 has already occurred during the discharge process and they are inevitable regardless of the use of RM which have little influence in the discharge process as shown in Supplementary Fig. 16. Actually, it is well-known that the current state of Li-O_2 battery is facing a big hurdle of dealing with side reactions during discharge, where Li_2CO_3 and carbonate-based byproducts are formed due to the carbon contamination and electrolyte deterioration. In particular, carbon-based electrode is more vulnerable to the formation of Li_2CO_3 upon deposition of Li_2O_2 discharge product on the surface of the carbon electrode, which leads to a decreased charging efficiency. [J. Phys. Chem. Lett. 3, 997 (2012)] Even though the gold and TiO_2 electrodes have been suggested as substitutional electrodes, other problems still persist such as the low energy density. In this respect, to avoid the formation of undesirable discharge products and clearly verify the intrinsic efficiency of RMs with Li_2O_2, we used commercialized Li_2O_2 powder in our experiment (Figure 3).

One thing that is worthy to note is that, in spite of the similar oxygen efficiency between the two cells, the use of DMPZ could reduce CO_2 evolution during charging compared to the cell without DMPZ. The Li-O_2 cell with DMPZ evolved only one third of CO_2 (1.02 μ mole)

DOI: 10.1038/NENERGY.2016.66

compared to the cell without DMPZ (3.44 μ mole). The decreased CO_2 evolution is attributable to the reduced charge polarization which lowers the charging voltage of the cell. It has been known that the carbon corrosion is accelerated in the high voltage charging above 3.5 V, where the primary source of carbon in the CO_2 evolution is the carbon electrode[J. Am. Chem. Soc. 135, 494-500 (2012)].

Supplementary Note 9. Discrepancy between experimental and calculated voltages.

Experimental potential data for Supplementary Table 2 were taken from Figure 2b in the manuscript, while calculated potential data were predicted from ionization energy and HOMO level of molecules. The discrepancy among redox potentials from the three methods was ~0.3 V, which is attributed to intrinsic DFT errors, e.g. spin contamination, the correlation effect of electrons in molecular orbital, implicit solvation assumption, etc. [Cramer, C. J. Essentials of Computational Chemistry: Theories and Models., 2nd edn. Wiley, 2014.]

While the discrepancy of the first redox potential between calculation and experiment was within ~0.3 V, the calculated second ionization potential of DMPZ was notably higher than the experimental value (~4.1 V). This discrepancy can be attributed to the particularly strong interaction of $DMPZ^{2+}$ with salt anions in the electrolyte, which was neglected in the HOMO calculation. The high valent $DMPZ^{2+}$ ion has the stronger interaction with salt anions and can be stabilized lowering the redox potential.

DOI: 10.1038/NENERGY.2016.66

Supplementary References

[1] Khetan A, Pitsch H & Viswanathan V. Solvent Degradation in Nonaqueous Li-O2 Batteries: Oxidative Stability versus H-Abstraction. J. Phys. Chem. Lett., 5, 2419-2424 (2014).

[2] Gritzner G. "Standard electrode potentials of M+|M couples in non-aqueous solvents (molecular liquids)" J. Mol. Liq., 156, 103 (2010)